20th Australasian Fluid Mechanics Conference
Perth, Australia
5-8 December 2016

Study on Multiphase Buoyancy-Drag Model of Mixing Induced by Rayleigh-Taylor Instability in Dusty Gases

M. Yang[1], L.L. Wang[1, 2] and S.D. Zhang[1, 2]
[1]The Institute of Applied Physics and Computational mathematics, Beijing 100094, China
[2]Center for Applied Physics and Technology, Peking University, Beijing 100871, China

Abstract

The evolutions of the material interpenetration boundary induced by Rayleigh-Taylor instability were calculated under various acceleration histories using a buoyancy-drag model. It reveals that the development of mixing under constant acceleration is very different from that under variable acceleration. The calculation results were compared with detailed experimental data to prove the validation of the model. On the bases of these, a multiphase buoyancy-drag model was developed to study mixing induced by Rayleigh-Taylor instability in dusty gases under constant acceleration. It is found that the mixing width decreases with the increase of the dusty concentration and the size of particles, which reveals that the particles in dusty gases restrain the development of mixing.

Introduction

When fluids of different densities are subjected to the acceleration which is in the opposite direction to the density gradient, Rayleigh-Taylor instability (RTI) occurs [7, 11]. Light fluid interpenetrates to heavy fluid to form bubbles, while heavy fluid interpenetrates to light fluid to form spikes. RTI plays an important role in natural phenomena and industrial applications, such as combustion, inertial confinement fusion (ICF), supernova explosion and geophysics et al. [3, 9].

When random perturbations on unstable interfaces are multimode spectrum, smaller structures compete and merge to form larger structures. This is an inverse cascade process. Until now, the theoretic study, numerical simulation and experimental investigation of RTI have been achieved a lot of useful information. It is found that the width of turbulent mixing zone (TMZ) increases with t^2 [2, 9], which can be used to validate the model of RTI in the case of multimode perturbations. Now single-phase buoyancy-drag model is used in engineering design to instead of empirical expression, and better results are obtained. But the pure gases are rare in engineering applications, and particle/ dust loading effects in gases often exist. In order to describe the effect of particles on mixing, a multiphase buoyancy-drag model is developed on the basis of its single-phase version, then it is used to study the evolution of RTI in dusty gases under constant acceleration and investigate the effects of particle loading N and particle size r_p on mixing.

In this paper the single-phase buoyancy-drag model is briefly described firstly. Secondly the multiphase buoyancy-drag model is developed. Then using this model, the mixing induced by RTI in dusty gas under constant acceleration is investigated. It is found that the mixing width decreases with the increase of the dusty concentration and the size of particles, which reveals that the particles in dusty gases restrain the development of mixing.

Model Equations and Numerical Algorithm

Single-phase Buoyancy-drag Model

Layzer is the first to predict RTI evolution successfully using potential flow model and obtain the original buoyancy-drag model describing bubble motion [4]:

$$du_B/dt = g(t)\cdot(1-E)/(2+E) - \left(u_B^2/\lambda\right)\cdot 6\pi/(2+E) \quad (1)$$

where E=exp(-6πa/λ).

Now the general buoyancy-drag model can be written as [10]:

$$\left[(C_a E(t)+1)\rho_1 + (C_a + E(t))\rho_2\right]\frac{du_B}{dt} = (1-E(t))(\rho_2-\rho_1)g(t) - C_d\rho_2\frac{u_B^2}{\lambda} \quad (2)$$

$$\left[(C_a E(t)+1)\rho_2 + (C_a + E(t))\rho_1\right]\frac{du_S}{dt} = (1-E(t))(\rho_2-\rho_1)g(t) - C_d\rho_1\frac{u_S^2}{\lambda} \quad (3)$$

where u_B and u_S denote the velocities of the bubbles and spikes respectively, g(t) is the time varying interface acceleration, and λ is the perturbation wavelength. C_a and C_d denote the added mass and bubble or spike drag coefficients respectively. These equations state that the net acceleration or deceleration of a bubble or spike is the difference between the buoyancy and drag forces acting. The left-hand side represents the total inertial of the bubble or spike and the inertial of the added mass which refers to the mass of the fluid that is pushed by the rising bubble or falling spike. In addition, the parameter $E(t)=e^{-C_e k h_B}$ is introduced to account to the amplitude dependence, where k (=2π/λ) is the wave number and h_B is the width of bubbles.

For multimode perturbations, we assume that bubbles and spikes have the same periodicity, so they have the same characteristic wavelength $\hat{\lambda}$. During the early linear growth regime, $\hat{\lambda}$ remains constant, but during the late time asymptotic regime, $\hat{\lambda}$ grows in a self-similar fashion, i.e., in proportion to the bubble amplitude h_B. Thus in the model $h_B/\hat{\lambda}$ =b(A), where b(A)=0.5/(1+A) and A=(ρ2-ρ1)/(ρ1+ρ2). The characteristic wavelength for multimode perturbations grows as:

$$\frac{d\hat{\lambda}}{dt}=\begin{cases}0, & h_B<\hat{\lambda}b(A)\\ \dfrac{u_B}{b(A)} & h_B\geq\hat{\lambda}b(A)\end{cases} \quad (4)$$

Under this assumption, only after the bubble amplitude h_B has reached the value $\hat{\lambda}b(A)$, $\hat{\lambda}$ starts to increase through bubble competition.

Multiphase Buoyancy-drag Model

The single-phase model in last section is now extended to account for multiphase effects. The basic formulation stems from the dusty gas studies of Saffman (1962) [8], Michael (1964) [5] and Ukai et al. (2010) [12]. Saffman applied the formulation to laminar flow by deriving the multiphase Orr-Sommerfeld equation; Michael extended this work to the study of plane Poisuelle flow of dusty gases; and Ukai et al. applied the formulation to two kinds of dusty gas Richtmyer-Meshkov instabilities. Here, the effect of dust is described by two parameters: the dust concentration (or number density N) and a relaxation time (essentially Stokes number St).

Recalling the formation of Saffman (1962) [8] and Ukai et al. (2010) [12], small perturbations are considered for flow variables and the governing equations are linearized. Then the above references apply boundary conditions at the far-field and at the species interface, following which the first order general expression applicable for RTI involving dusty gases is obtained as:

$$\rho_1\left[1+\frac{f_1}{1-ik\tau_1 c}\right]\left(g-kc^2\right)=\rho_2\left[1+\frac{f_2}{1-ik\tau_2 c}\right]\left(g+kc^2\right) \quad (5)$$

where f_1 and f_2 denote the particle mass loading in the light and heavy gases respectively and evaluated as $f_1=mN_0/\rho_1$ and $f_2=mN_0/\rho_2$, where m is the dust particle mass, and N_0 is the initial dust concentration in number per unit volume. The other terms in equation (5) represent the acceleration g(t), wave number k, wave speed c, particle relaxation time scale τ (subscripts 1 and 2 correspond to fluids 1 and 2 respectively), and I is the complex number $(-1)^{1/2}$. The relaxation times are obtained as $\tau_1=\tau_2=m/(6\pi r_p\mu)$. In this paper we assume $\tau_1=\tau_2$, which need not necessarily be always true, the other assumption made is that Stokes drag is valid. Thus equation (5) can also be written as:

$$\rho_1\left[1+\frac{f_1}{1+St_1}\right]\left(g-kc^2\right)=\rho_2\left[1+\frac{f_2}{1+St_2}\right]\left(g+kc^2\right) \quad (6)$$

where $St_1=St_2=-ik\tau c$ is assumed in this study. Furthermore, Ukai et al. (2010) define a multiphase Atwood number A_m under the small St (<<1) limit as:

$$A_m=\frac{\rho_2(1+f_2)-\rho_1(1+f_1)}{\rho_2(1+f_2)+\rho_1(1+f_1)} \quad (7)$$

which, for a generic St, can be written as:

$$A_m=\frac{\rho_2\left(1+\left(f_2/(1+St_2)\right)\right)-\rho_1\left(1+\left(f_1/(1+St_1)\right)\right)}{\rho_2\left(1+\left(f_2/(1+St_2)\right)\right)+\rho_1\left(1+\left(f_1/(1+St_1)\right)\right)} \quad (8)$$

Thus the multiphase effect in the formation leads to the extension of the classical Atwood number A to the multiphase Atwood number Am as defined in equation (8). In addition, ρ is replaced by $\rho(1+f/(1+St))$ in the multiphase formulation. Following equations (2) and (3) by considering the added mass term, buoyancy and drag effects, we can analogously and intuitively obtain the following two equations for the bubble and spike motion in dusty gases:

$$\left[\left(C_a E(t)+1\right)\rho_1^m+\left(C_a+E(t)\right)\rho_2^m\right]\frac{du_B}{dt}=\left(1-E(t)\right)\left(\rho_2^m-\rho_1^m\right)g(t)-C_d\rho_2^m\frac{u_B^2}{\lambda} \quad (9)$$

$$\left[\left(C_a E(t)+1\right)\rho_2^m+\left(C_a+E(t)\right)\rho_1^m\right]\frac{du_S}{dt}=\left(1-E(t)\right)\left(\rho_2^m-\rho_1^m\right)g(t)-C_d\rho_1^m\frac{u_S^2}{\lambda} \quad (10)$$

For multimode perturbations, we extend equation (4) by also accounting for multiphase effects through the $b(A_m)$ parameter, defined as $b(A_m)=0.5/(1+A_m)$ and also appropriately modify the characteristic wavelength for multimode perturbations to account for multiphase effects:

$$\frac{d\hat{\lambda}}{dt}=\begin{cases}0, & h_B<\hat{\lambda}b(A_m)\\ \dfrac{u_B}{b(A_m)} & h_B\geq\hat{\lambda}b(A_m)\end{cases} \quad (11)$$

Here we are using the same definitions for $\hat{\lambda}$, with the only replacement for A by A_m.

Numerical Algorithm

For single-phase model, equations (2) and (3) are solved. In the case of multimode perturbations, equation (4) is also solved. For multiphase model, equations (9) and (10) are solved. In the same it is needed to solve equation (11) for multimode perturbations. Thus the model equations solved in this study are a set of second order ordinary differential equations which can be transformed to first order difference equations as $dh_{B,S}/dt=u_{B,S}$ and $du_{B,S}/dt=C_1 g-C_2 C_d u_{B,S}^2/\lambda$. They can be solved by forth order Runge-Kutta method.

Results Analysis and Discussion

Validation of the Single-phase Buoyancy-drag Model

This section is to validate the single-phase model. The widths of bubble and spike under four kinds of accelerations (see figure 1) are calculated using this single-phase mode. In figure 1, four kinds of acceleration which are experimental data measured by Dimonte et al. [2] are denoted as G_n, n=1,2,3,4, and g_0 is the gravity acceleration. In the calculation, good agreement can be obtained by adjusting drag coefficient C_d and initial amplitude h_{i0}.

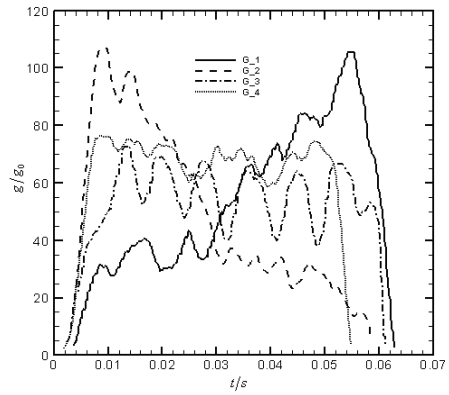

Figure 1. Four kinds of accelerations used in the calculation.

The widths of bubble and spike versus displacement Z are given in figure 2 and 3. Here, $Z=\iint gdt'dt$. From these two figures, it can be seen that under four kinds of accelerations the calculated values of widths of bubble and spike are agreed to their experimental values. In addition, widths of bubble and spike are evidently dependent to the slope dg/dt. If dg/dt>0, the mixing is enhanced, while if dg/dt<0, the mixing is decreased, which shows that the increasing acceleration is the most unstable acceleration profile. This could be important to ICF [1]. In the calculation, the ratio of densities of two fluids is small, during instability development process the asymmetry of bubble and spike is not evident, so the difference between widths of bubble and spike is small.

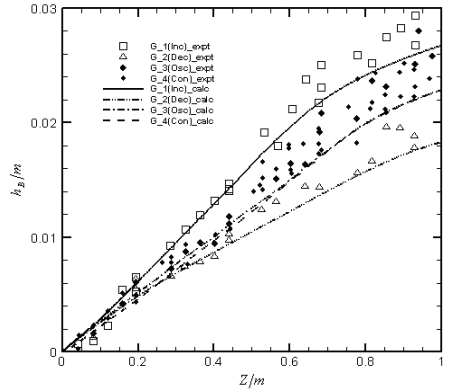

Figure 2. The width of bubbles versus the displacement Z.

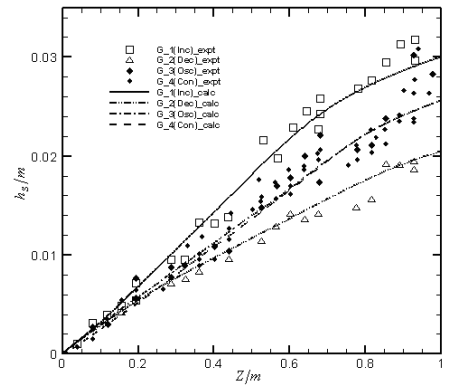

Figure 3. The width of spikes versus the displacement Z.

Study on RTI in Dusty Gases Using the Multiphase Buoyancy-drag Model

In this section, the effect of solid particles on the RT mixing layer growth in dusty gases is investigated, first for single-mode RT, and then for multimode RT. The emphases of our study are the effects of particle loading N and particle size r_p. We apply the multiphase buoyancy-drag model for cases corresponding to A=0.5, ρ_1=1kg/m^3, ρ_2=3kg/m^3, g=1m/s^2, initial wavelength λ_0=1cm and initial amplitude a_0=0.1mm.

For single-mode perturbations, we first investigate the effect of N on the amplitude growth. r_p=40μm is chosen and this corresponds to St~1. We consider a baseline particle-free (N=0) case in addition to N in the range 10^8-10^{13}m^{-3}. Figure 4 shows the non-dimensional amplitude ka (where $a=0.5(h_B+h_S)$) versus non-dimensional time $((A_m kg)^{1/2}t)$. As expected, ka grows slower for higher N, since particles serve as an obstruction to the bubble and spike motion. We also compute the late time slopes of the bubble and spike amplitudes to obtain the respective late time constant bubble and spike terminal velocities ($U_{RT(B/S)}$). The multiphase buoyancy-drag model predictions for $U_{RT(B/S)}$ are in accordance with the value obtained by equating the buoyancy and drag terms:

$$U_{RT(B/S)} = \sqrt{\left(2A_m/\left(1 \pm A_m\right)\right)\left(g\lambda/C_d\right)} \qquad (12)$$

consistent with the results obtained by Oron et al. (2001) [6], albeit with A_m in place of A (the + sign corresponds to the bubbles and the – sign for the spikes). In addition, it is interesting to note in figure 4 that as N increases, the non-dimensional profiles also tend to converge, thereby creating a band of solutions between $A_m \rightarrow A$ and $A_m \rightarrow 0$.

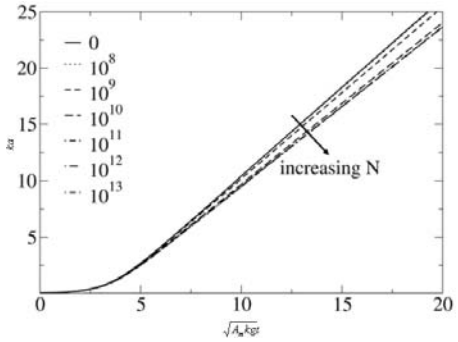

Figure 4. Non-dimensional amplitude versus non-dimensional time for different particle loadings with r_p=40μm in single-mode RTI.

Next, we study the effect of r_p for a fixed N=10^{10}m^{-3}. We consider particle size in the range r_p=4-400μm, corresponding to different St. Here r_p=4μm corresponds to St~0.01, r_p=40μm to St~1 and r_p=400μm to St~100. Figure 5 shows the non-dimensional amplitude versus non-dimensional time. It can be seen that ka grows slower for higher N. In addition, for very small r_p, little particle mass is present to influence bubble and spike motion, so the results conform to the particle-free case (A_m=A). On the other hand, for very large particle sizes, $1+f/(1+St) \rightarrow 6\pi r_p \mu N/\rho$, so $1+f/(1+St) \rightarrow 6\pi r_p \mu N$, i.e., independent of ρ. Hence the initial density ratio loses significance and the mixing layer evolves tending to the $A_m \rightarrow 0$ limit.

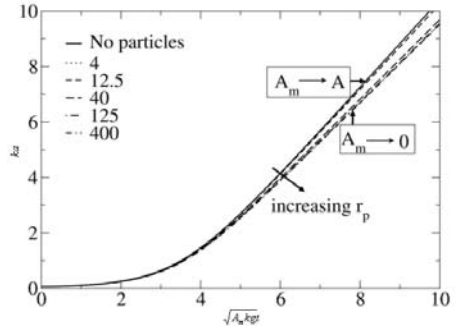

Figure 5. Non-dimensional amplitude versus non-dimensional time for different particle sizes with N=10^{10}m^{-3} in single-mode RTI.

For multimode perturbations, the same initial conditions are used, with the difference being the use of $\hat{\lambda}$ instead of λ and the corresponding equation for the wavelength growth rate (equation (11)). Figure 6 displays the growth of amplitude versus $A_m g t^2$ for a fixed r_p=40μm for a range of N. As evident, higher N results in subdued mixing layer amplitude growth as more particles obstruct the rise of bubbles and the fall of spikes. Again the results are contained within a band, with the upper limit corresponding to $A_m \to A$ (for $N \to 0$) and the lower limit to $A_m \to 0$ (for $N \to \infty$). The slope of these curves α are evaluated to be α=0.0606 for the upper limit and α=0.0491 for the lower limit. These values are similar to the classical result of α~0.05 reported by Youngs [13-16]. Thus it is possible that some of the established theories on hydrodynamic instability growth can be extended to multiphase systems as well by replacing A with A_m.

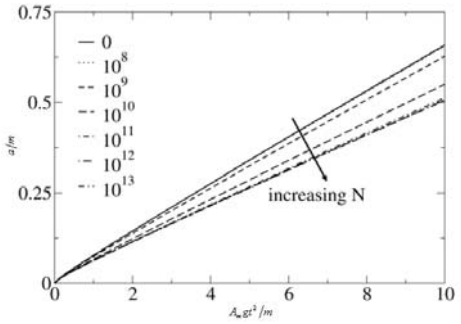

Figure 6. Non-dimensional amplitude versus $A_m g t^2$ for different particle loadings with r_p=40μm in multimode RTI.

Next we fix the particle loading at 1011m-3 and vary particle sizes in the range r_p=4-400μm for the same initial conditions. Figure 7 shows the amplitude variation versus $A_m g t^2$. As evident, linear trends (in t^2) are observed at later times, with the amplitude contained within a band. Furthermore, as particles obstruct the evolution of the mixing layer, the amplitude increases slowly with the increase of particle sizes.

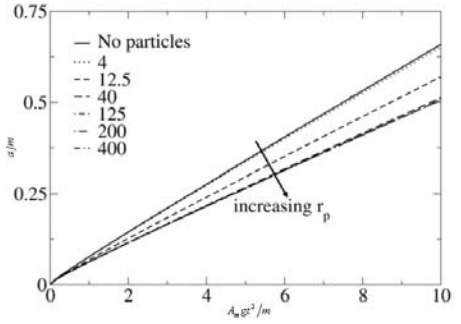

Figure 7. Non-dimensional amplitude versus $A_m g t^2$ for different particle sizes with $N=10^{10} m^{-3}$ in multimode RTI.

Conclusions

In this study, multiphase buoyancy-drag model is developed on the basis of its single-phase version. The single-phase buoyancy-darg model is validated by the comparison with the experimental results. Then the RT mixing in dusty gases under constant acceleration is investigated using the multiphase model. It is found that the mixing width decreases with the increase of the particle number density and the size of particles, which reveals that the particles in dusty gases restrain the development of mixing.

Acknowledgments

This work is supported by the scientific technology development fund of the Agency of Chinese Engineering Physics (No. 2015B0201038).

References

[1] Chen B., Modeling chaotic mixing, *Nuclear Weapons Journal*, 1, 2010, 8-17.

[2] Dimonte G. & Schneider M., Density ratio dependence of Rayleigh-Taylor mixing for sustained and impulsive acceleration histories, *Physics of Fluids*, 12(2), 2000, 304-321.

[3] Hansom J. C. V., Rosen P. A., Goldack T. J., Oades K., Fieldhouse P., Cowperthwaite N., Youngs D. L., Mawhinney N. & Baxter A. J., Radiation driven planar foil instability and mix experiments at the AWE HELEN laser, *Laser and Particle Beams*, 8(1), 1990, 51-71.

[4] Layzer D., On the gravitational instability of two superposed fluids in a gravitational field, *Astrophysics Journal*, 122, 1955, 1-17.

[5] Michael D. H., The stability of plane Poisuelle flow of a dusty gas, *Journal of Fluid Mechanics*, 18, 1964, 19-21.

[6] Oron D., Arazi L., Kartoon D., Rikanati A., Alon U. & Shvarts D., Dimensionality dependence of the Rayleigh-Taylor and Richtmyer- Meshkov instability late-time scaling laws, *Physics of Plasmas*, 8, 2001, 2883-2889.

[7] Rayleigh L., Investigation of the character of the equilibrium of an incompressible heavy fluid of variable density, *Proceedings of the London Mathematical Society*, 14, 1883, 170-177.

[8] Saffman P. G., On the stability of laminar flow of a dusty gas, *Journal of Fluid Mechanics*, 13, 1962, 120-128.

[9] Sharp D. H., An overview of Rayleigh-Taylor instability, *Physica D*, 12, 1984, 3-18.

[10] Srebro Y., Elbaz Y., Sadot O., Arazi L. & Shvarts D., A general buoyancy-drag model for the evolution of Rayleigh-Taylor and Richtmyer-Meshkov instabilities, *Laser and Particle Beams*, 21, 2003, 347-353.

[11] Taylor G., The instability of liquid surfaces when accelerated in a direction perpendicular to their planes Ⅰ, *Proceedings of the Royal Society of London*, A201, 1950, 192-196.

[12] Ukai S., Balakrishnan K. & Menon S., On the Richtmyer-Meshkov instability in dilute gas-particle mixtures, *Physics of Fluids*, 22, 2010, 104103.

[13] Youngs D. L., Numerical simulation of turbulent mixing by Rayleigh- Taylor instability, *Physics D*, 12, 1984, 32-44.

[14] Youngs D. L., Modelling turbulent mixing by Rayleigh-Taylor instability, *Physics D*, 37, 1989, 270-287.

[15] Youngs D. L., Three-dimensional numerical simulation of turbulent mixing by Rayleigh-Taylor instability, *Physics of Fluids*, A3, 1991, 1312-1320.

[16] Youngs D. L., Numerical simulation of mixing by Rayleigh-Taylor and Richtmyer-Meshkov instabilities, *Laser Particle Beams*, 12, 1994, 725-750.